

Pattern Classification of Human Cognitive State in Man-Machine Systems Using Multiple Sources of Psychophysiological Data and Fuzzy Clustering Approach

Jian-Hua Zhang*

*Department of Automation, East China University of Science and Technology, Shanghai 200237, P.R. China (Tel: ++86-21-64253808; e-mail: zhangjh@ecust.edu.cn)

Abstract: The primary goal of this work is to classify Human Cognitive State (HCS) in human-machine cooperative control systems. A total of 10 young and fit volunteers were used as the experimental subjects. A set of 9 process control task conditions were programmed on an automation-enhanced Cabin Air Management System (aCAMS) originally developed to simulate with high-fidelity the life support system in aerospace applications. The psychophysiological and performance data of the subjects were recorded while they performed process control operations in collaboration with computer-based automatic control systems. The fuzzy C-Means (FCM) algorithm was used to classify the momentary HCSs into three categories: "Good", "Average" and "Risky" with certain degree of membership. The classification results indicated that the FCM-based classifier can achieve accurate HCS classification if the influential features are properly selected. The method proposed has potential to be applied to design adaptive task (or functional) allocation strategy in adaptive/intelligent human-machine control systems.

1. INTRODUCTION

The rapid development of automation technologies in the past decades has resulted in the replacement of manual labor by automated systems as well as the shift of the role of the human from manual operator to the monitor or supervisor of various automation systems. Therefore, more demanding requirements on the mental capability and resources of humans are imposed although the physical demands are somehow reduced. In the safety-critical systems arising from such diverse industry as aviation, space, railway and nuclear power, humans normally play the role of monitoring/supervision and decision-making. The human performance in those systems plays a pivotal role in the overall performance of the human-machine system as a whole. Once human performance breakdown occurs, the man-machine system would severely malfunction or breakdown. In order to maintain the safety of these systems, human performance must be quantitatively investigated. Therefore, the studies on the impact of Mental WorkLoad (MWL) on work performance are essential to enhance the safety and productivity (Hockey, 1997; Wilson and Fisher, 1995; Hanskins and Wilson, 1998; Wilson and Russell, 1999).

Although human operator usually can achieve higher-level task goals by investing more efforts and use of risky strategies, s/he is likely to be in a vulnerable (or high-risk) cognitive state well prior to explicit performance decrement.

In the risky state, the operator can still deal with the foreseeable demands, but cannot respond promptly to those unforeseeable or difficult events, which may lead to serious consequences (Hockey, 1997). To avoid severe accidents caused by the decrement in human performance, human cognitive state (HCS) must be evaluated and then used to allocate adaptively the tasks between human and machine parts in the integrated system with an aim to achieve optimal performance of the two integral components.

The basic objective of the present investigation is to find a way to objectively and accurately recognize/identify HCS that may fluctuate over time. The paper is organized in the following structure. The experimental collection of the psychophysiological and performance data (such as Heart Rate (HR), electroencephalogram (EEG) and other measures) from 10 subjects is first described. Then the extraction of the most salient subject-specific features of the HCS is discussed. Finally the results of use of Fuzzy C-Means (FCM) algorithm to classify the HCS data are presented and analyzed, followed by some meaningful conclusions drawn.

2. DATA ACQUISITION EXPERIMENTS

The automation-enhanced Cabin Air Management System (aCAMS) was adopted to simulate a complex, safety-critical, multi-variable, and multi-task process control environment. This would overcome the drawbacks of most previous work that often used over-simplified task patterns in their studies.

The aCAMS software platform, whose function modules are shown in Fig. 1, was initially developed for European Space Agency (ESA) to study the level and stressors of stress or strains imposed on the astronauts under highly separated and confined work and living environment (Hockey, 1997).

The operator subject was required to maintain such air quality indices as CO₂, oxygen, pressure, temperature, and humidity within normal ranges. The levels of task difficulty were varied across different task conditions by changing gradually (stepwise) the number of variables requiring manual control by the operator. The physiological (ECG, EEG, etc.) data were simultaneously recorded while the operator performs the control tasks assigned in each task condition.

A total of 10 college student subjects, all with engineering majors, were used in our experiments. Before the formal experiments started, in manual mode of aCAMS each subject had taken over 10 hrs to get himself familiarized to the aCAMS software platform as well as the simulated control tasks. Each subject was asked to participate in 2 sessions of experiment, each of which was arranged at the same time-period but at different days so as to avoid the effects of circadian rhythms. The experimental session lasted for about 135 mins with 9 consecutive task conditions, each lasting for about 15 mins with different level of task difficulty. The subjective ratings were performed between 2 conditions, lasting for about 20 sec. Right after the health questionnaire and subjective ratings, the control tasks were started up. In addition to the ECG and EEG data, the work performance data of the subject were also recorded.

The EEG data were measured by using 32 electrodes which was configured according to the standard international 10-20 electrode placement system. The EEG data sampling rate is preset as 2048 Hz. The band-pass filter with a passing band between 1.6 and 55 Hz were used to preprocess the EEG signals. The data preprocessing was completed on the BioSemi system. After preprocessing procedures, we obtained the HR data every second, EEG data every 2 seconds, and primary-task performance data (i.e., *time-in-range*) every second.

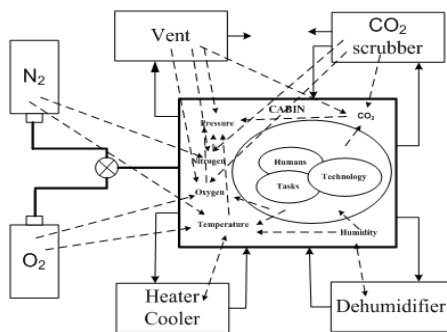


Fig. 1. The functional configuration of an aCAMS.

3. DATA PREPROCESSING AND ANALYSIS

The measured data (including ECG, EEG, etc.) needs to be preprocessed before appropriate HCS feature selection

(Zhang *et al.*, 2008a, b). In this paper, we finally selected 4 significant features, namely *HR*, *HRV₂*, *TLL₁*, *TLL₂*, which are shown to be more sensitive to the variations in task load. The 4 important features of the HCS are first introduced in the following.

HR represents the mean value of HR within a sampling interval (i.e., 1 min). *HRV₂* is the ratio of the standard deviation and mean of HR data within a sampling interval (i.e., 1 min) and defined by (Zhang *et al.*, 2008a, b):

$$HRV_2 = \frac{\sigma_{HR}}{\mu_{HR}} \quad (1)$$

TLL₁ and *TLL₂* are two EEG-based Task Load Indices (TLI) defined as the ratio of theta and alpha band powers of the EEG signals measured from certain electrodes placed on different regions of the scalp, i.e.,

$$TLL_1 = \frac{P_{\theta, Fz}}{P_{\alpha, Pz}} \quad (2)$$

$$TLL_2 = \frac{P_{\theta, AFz}}{P_{\alpha, CPz-POz}} \quad (3)$$

where Fz, Pz, AFz, CPz, and POz stand for 5 EEG electrodes in international 10-20 system, respectively; θ (4-8Hz), α (8-13Hz), and β (13-22Hz) are the commonly-divided EEG frequency bands corresponding to different rhythms inherent in the EEG signal; and *TIR* is derived from the data of *system-in-deviation* and represents the percentage of the time, during which the primary task performance lies within the normal range pre-specified.

There are all together 10 subjects, each performing 2 sessions of data collection experiment. Each session lasted for about 135 min (=15 min / condition * 9 conditions). Due to the short period (around 0.5 min) of subjective ratings and presetting of different task conditions, we discarded the first and last 0.5 min data in each task-load condition, in this way there is 14-min data in each task-load condition. After down-sampling the measured data to 1 Hz, we finally obtain 126 (= 14 points / condition * 9 conditions) data points in each session of dataset. In our work, the sample data from the 1st session (s1 in short will be used hereafter) will be used for

training the fuzzy classifier, while the 2nd session (s2 in short will be used hereafter) dataset for checking its generalization (or prediction) performance.

4. HCS CLASSIFICATION APPROACH AND RESULTS

In this section we will adopt Fuzzy C-Means (FCM) algorithm to classify the HCS data.

4.1 FCM algorithm

Depending on the nature of the problem, fuzzy recognition offers flexible modeling by extending the 0-1 membership to the membership in the interval of [0, 1] (Gustafson and Kessel, 1979). The use of fuzzy models also makes it easier to solve pattern recognition problems (Windham, 1982). Solving a non-fuzzy model usually involves an exhausted (or comprehensive) search in the whole space. Some key variables only take two discrete value of 0 or 1. In contrast, all variables in fuzzy models are continuous and the gradient computing can be performed to find the optimal search direction. The key problem of fuzzy recognition is to find the respective classes assigned to a series of data. One of the most well-known fuzzy clustering approaches is the FCM algorithm (Pal and Bezdek, 1995). With FCM the membership degree with which a data point belongs to a certain cluster can be obtained, which offers a new approach to mapping the data in higher-dimensional feature space onto a set of clusters (Krishnapuram and Keller, 1996). The task of FCM algorithm is to find the membership degree matrix U and cluster center matrix V to minimize

$$J_m(U, V) = \sum_{k=1}^n \sum_{i=1}^c (u_{ik})^m \|\mathbf{x}_k - \mathbf{v}_i\|^2 \quad (4)$$

where $U = [u_{ik}] \in M_{fc}$ denotes the matrix of membership degrees, $V = (\mathbf{v}_1, \mathbf{v}_2, \dots, \mathbf{v}_c)$, $\mathbf{v}_i \in R^p$ with \mathbf{v}_i the center of the i -th cluster, and $m \in (1, \infty)$ is the weighting exponent.

The computational procedure of FCM algorithm consists of the following 4 steps:

Step 1: Preset $c \in \{2, 3, \dots, n-1\}$ and $m = 2$ and initialize

$$U^{(0)} \in M_{fc}.$$

Step 2: At the l -th iteration, cluster centers are computed by:

$$\mathbf{v}_i^{(l)} = \frac{\sum_{k=1}^n (u_{ik}^{(l)})^m \mathbf{x}_k}{\sum_{k=1}^n (u_{ik}^{(l)})^m}, 1 \leq i \leq c; l = 0, 1, 2, \dots \quad (5)$$

Step 3: $U^{(l)} = [u_{ik}^{(l)}]$ is updated to $U^{(l+1)} = [u_{ik}^{(l+1)}]$ by:

$$u_{ik}^{(l+1)} = \frac{1}{\sum_{j=1}^c \left(\frac{\|\mathbf{x}_k - \mathbf{v}_i^{(l)}\|}{\|\mathbf{x}_k - \mathbf{v}_j^{(l)}\|} \right)^{\frac{2}{m-1}}}, 1 \leq i \leq c; 1 \leq k \leq n \quad (6)$$

Step 4: If $\|U^{(l+1)} - U^{(l)}\| < \varepsilon$ (small constant), the algorithm would stop; otherwise assign $l \leftarrow l+1$ and loop back to *Step 2*.

4.2 Results and discussion

The HCS of each subject was classified by using the FCM into three classes with their corresponding labels c1 (*Good*), c2 (*Average*), and c3 (*Risky*). For each subject, there are two datasets (measured from s1 and s2, respectively), each consisting of 126 data points. The s1 dataset was classified, then the s2 dataset was done again. In this way, the Classification Consistency Rate (CCR) between two sessions of dataset can be computed. In the FCM, the Membership Degree (MD) and cluster center matrices are first randomly initialized. The initialized MDs give the grades of membership, with which each data point belongs to some cluster. The initialized cluster centers predetermine the number and initial position of data clusters in the feature space. Following the initialization process, the FCM starts its iterative computing procedure. Finally, in order to obtain a crisp classification label, the class with the maximum MD is selected as the class, to which a data point belongs.

First all the data was normalized to the range between 0 and 1. The 1st and 2nd-session dataset were clustered by the FCM, respectively, using the same initialization parameters (i.e., the MD and cluster center matrices). The CCR was then defined as the percentage of the time-series data, which get the same classification label at certain time instant in both s1 and s2. In Table 2, the first row is the 2D features with 4 possible combination of variables, namely (*HR, TIR*), (*HRV₂, TIR*),

(TLL_1, TIR), and (TLL_2, TIR) and the first column corresponds to individual subjects. The data whose CCR is higher than 60% are shown in bold font. The same computational approach is used for other 9 subjects. The CCRs for all subjects are then summarized by Table 2, from which obvious inter-subject difference can be easily detected, for instance the best classification performance (i.e., $CCR > 60\%$) was achieved for subjects F and J while much worse for subjects D and H.

Now consider using the 2D feature (HR, TIR) as the input of the fuzzy classifier for subject F. The feature plane of the 1st- and 2nd-session dataset is shown in Fig. 2a) and 2b), respectively, where the red marks give the three cluster centers. The comparison of the classification results based on s1 and s2 dataset is illustrated in Fig. 3a), where s1 and s2 data points are marked with squares and circles, respectively. It can be seen that most data points which are classified to c1 lie at the beginning and final time intervals, whereas those belonging to c2 and c3 are distributed in the middle part of the time axis. The more detailed classification results for subject F were summarized by Table 1, from which it is seen that 9.5% number of data points correspond to the risky operator state, whereas more than 90% *Average* or *Good* state and that over a half of the data points in both s1 and s2 were classified into c1. These results agree well with the phenomenon that there are a large number of nearly perfect TIR (i.e., near or equal to 1) data points in both s1 and s2. Furthermore, it seems that the classification of data points from s1 and s2 is more consistent in c3 than in other two classes. Due to the border (or boundary) between c1 (*Good*) and c2 (*Average*) is fuzzier in nature, it is intuitively natural that it may be more difficult to discriminate the two classes. The comparison of the class MDs due to s1 and s2 dataset is shown in Fig. 3b), in which most MDs are larger than 0.5 and most MDs assigned with c1 are especially higher (quite a few even reach 1, implying the classification results with complete degree of belief). The computed CCR for subject F reaches 69.05%.

Next, consider the Task-Load Level (TLL) as another supplementary feature and combine it with TIR to constitute a 2D feature vector. According to our special experimental design – cyclical loading scheme, the TLL was designed to vary from low to high, then from high to low, i.e., 1→2→

3→ 4→ 5→ 4→ 3→ 2→ 1, corresponding to a series of 9 task-load conditions each with certain TLL which can be quantified as the number of variables requiring manual control by the operator. Obviously the TLL can also be considered as an index of task difficulty for the operator.

The operator is usually in good functional (or cognitive) state, i.e., c1, under lowest TLL and in not-so-good state with other TLLs. The HCS classification results shown in Fig. 3a) agree well with this observation. Although the functional state of a subject may be somewhat different in two experimental sessions arranged at different days, under the same experimental conditions and procedures the CRR is still as high as nearly 70% for subject F, which initially demonstrated the feasibility and effectiveness of the FCM for the HCS classification. The classification procedure used is the same as above. It is seen that the CRR has been dramatically improved, for instance the lowest one is 72.22% for subject G and the highest one 100% for subject K. The results of HCS classification based on that 2D feature vector are shown to be very encouraging. Furthermore, let us concatenate the 2 session dataset of each subject into a new dataset, on which the FCM was used again. The classification results based on the concatenated dataset are shown by the last column of Table 2 to be better than those when using the s1 and s2 data separately. In summary, our results have demonstrated that the FCM-based method can achieve satisfactory HCS classification performance provided that the proper features are selected.

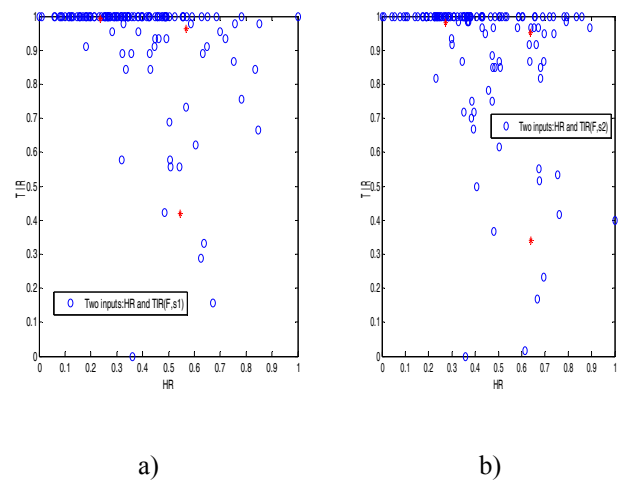


Fig. 2. Feature (HR and TIR) plane for subject F: a) s1; b) s2.

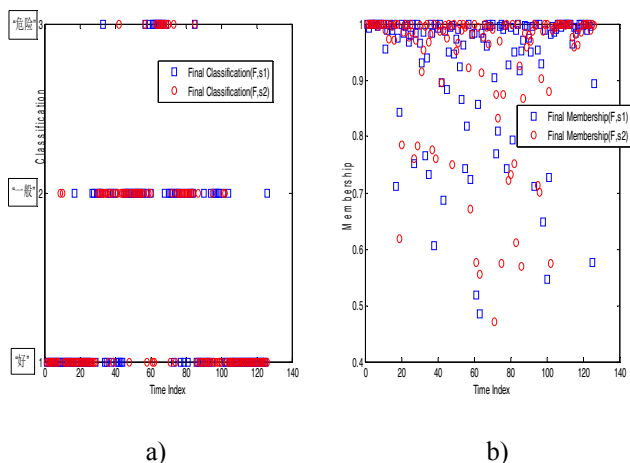


Fig. 3. Comparison of HCS classification results using the data from 2 sessions of subject F: a) class label; b) class MD.

Table 1. The results of the 3-class HCS classification based on 2 features (i.e., HR and TIR) for subject F.

Session #	c1 (Good)	c2 (Avg.)	c3 (Risky)
s1	69 (54.76%)	45(35.71%)	12 (9.52%)
s2	72 (57.14%)	42(33.33%)	12 (9.52%)

Table 2. Comparison of the FCM-based HCS classification performance (indexed by the CCR values) for all 10 subjects using different feature vector selected.

	(HR, TIR)	(HRV ₂ , TIR)	(TLI ₁ , TIR)	(TLI ₂ , TIR)	(TLL, TIR)	2TIR
A	0.3968	0.5318	0.4444	0.5238	0.9921	0.7619
C	0.4206	0.3175	0.5635	0.5159	0.8571	0.6349
D	0.3571	0.4206	0.6587	0.6429	0.8889	0.7222
E	0.3810	0.5318	0.5952	0.5476	0.8889	0.5873
F	0.6905	0.5873	0.5714	0.3889	0.7540	0.8968
G	0.5079	0.4444	0.4762	0.4048	0.7222	0.5397
H	0.2857	0.5079	0.4921	0.6349	0.8810	0.7302
J	0.6032	0.5238	0.5397	0.4841	0.7857	0.5476
K	0.5476	0.4444	0.3889	0.3254	1.0000	0.7540

L	0.5397	0.4206	0.4365	0.4444	0.8095	0.6746
---	--------	--------	--------	--------	---------------	---------------

If all the five candidate features, namely *HR*, *HRV2*, *TLI1*, *TLI2* and *TIR*, are used jointly for the classification of the momentary HCS into three classes, in the following the classification results for subject F (s1) will be presented. The five candidate features derived from the data from s1 and s2 are shown in Fig. 4a) and b), respectively. Each feature consists of 126 data points.

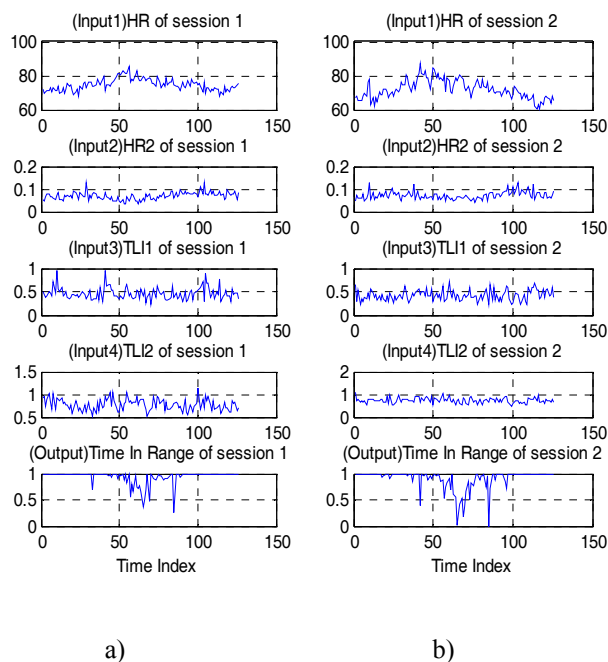


Fig. 4. The five candidate features vs time for subject F: a) s1; b) s2

The classification results for the s1-data of subject F are shown in Fig. 5 and Fig. 6, where the c1 (Good), c2 (Average) and c3 (Risky) are marked in blue, green and red, respectively. The three cluster centers ($\mathbf{v}_i \in \mathbb{R}^5, i = 1, 2, 3$) are given in Table 3.

Table 3. Centers of the three clusters (subject F; s1)

Cluster	<i>HR</i>	<i>HRV2</i>	<i>TLI1</i>	<i>TLI2</i>	<i>TIR</i>
c1-Good	71.0920	0.0742	0.5045	0.7786	0.9938
c2-Avg.	75.3002	0.0705	0.4332	0.7633	0.8892
c3-Risky	80.3072	0.0554	0.4545	0.7756	0.7823

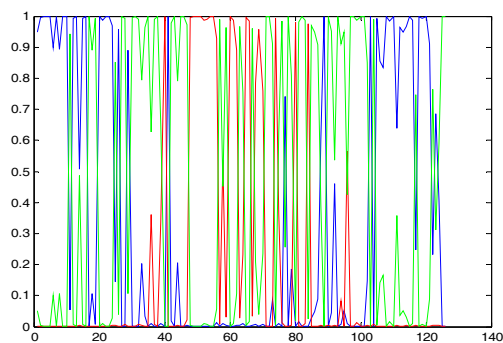


Fig. 5. The 3-class HCS classification results (subject F; s1).

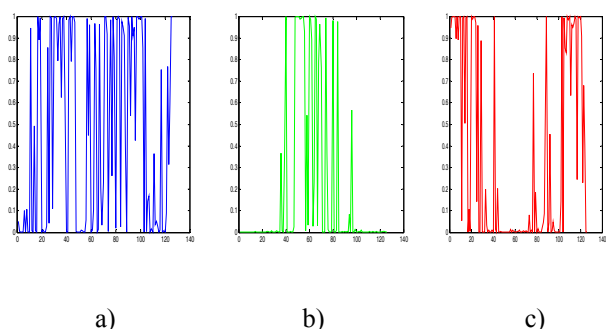


Fig. 6. The membership grades: a) class1; b) class2; c) class3.

5. SUMMARY AND CONCLUSIONS

The main goal of this work is to classify the HCS-related physiological to provide an objective basis for designing the AA-based human-machine systems. The HCS was classified into three classes, corresponding to *Good*, *Average* and *Risky* operator cognitive state.

The results reported have shown the effectiveness of the FCM-based method for the HCS classification if the proper (or influential) physiological features are selected. Moreover, significant individual difference across subjects was also observed from the results. Based on the quantitative assessment of the HCS, the cognition-demanding tasks can be adaptively allocated between human operator and machine agents so as to avoid the serious or even catastrophic consequences of operator cognitive function breakdown (Zhang et al., 2008a, b). In conclusion, the current work may provide a solid basis for implementing adaptive control of human-machine cooperative systems in safety-critical scenarios.

ACKNOWLEDGMENTS

This work was supported by the National Natural Science Foundation of China under Grant No. 61075070 and Key Grant No. 11232005.

REFERENCES

- Gustafson, D.E. and Kessel, W.C. (1979), Fuzzy clustering with a fuzzy covariance matrix, in *Proc of the IEEE-CDC*, San Diego, CA, pp. 761-766.
- Hanskins, T.C. and Wilson, G. F. (1998), A comparison of heart rate, eye activity, EEG and subjective measures of pilot mental workload during flight, *Aviation, Space, and Environmental Medicine*, Vol. **69** (4), pp. 360-367.
- Hockey, G.R.J. (1997), Compensatory control in the regulation of human performance under stress and high workload: A cognitive energetically framework, *Biological Psychology*, pp. 45-73.
- Krishnapuram, R. and Keller, J.M. (1996), The possibilistic c-means: Insights and recommendations, *IEEE Trans. on Fuzzy Systems*, Vol. **4**, pp. 385-393.
- Pal, N.R. and Bezdek, J.C. (1995), On cluster validity for the fuzzy c-means model, *IEEE Trans. on Fuzzy Systems*, Vol. **3** (3), pp. 370-379.
- Windham, M. P. (1982), Cluster validity for the fuzzy c-means clustering algorithm, *IEEE Trans. on Pattern Analysis and Machine Intelligence*, Vol. **4** (4), pp. 357-363.
- Wilson, G.F. and Fisher, F. (1995), Cognitive task classification based upon topographic EEG data, *Biological Psychology*, Vol. **40**, pp. 239-250.
- Wilson, G.F. and Russell, C.A. (1999), Operator functional state classification using neural networks with combined physiological and performance features, in *Proc. of 43rd Human Factors and Ergonomics Annual Meeting*, pp. 1099-1102.
- Zhang, J.-H., Wang, X.-Y., Mahfouf, M., Linkens, D.A. et al. (2008a), Use of heart rate variability analysis for quantitatively assessing operator's mental workload, in *Proc. of the Intl Conf. on Biomedical Engineering and Informatics (BMEI)*, Vol. **1**, pp. 668-672.
- Zhang, J.-H., Wang, X.-Y., Mahfouf, M., Linkens, D.A. et al. (2008b), Fuzzy logic based identification of operator functional states using multiple physiological and performance measures, in *Proc. of the Intl Conf. on Biomedical Engineering and Informatics (BMEI)*, Vol. **1**, pp. 570-574.